# Measurement of Regional Cerebral Glucose Utilization with Fluorine-18-FDG and PET in Heterogeneous Tissues: Theoretical Considerations and Practical Procedure

Giovanni Lucignani, Kathleen C. Schmidt, Rosa M. Moresco, Giuseppe Striano, Fabio Colombo, Louis Sokoloff and Ferruccio Fazio

*INB-CNR, Department of Nuclear Medicine University of Milan, Institute H. San Raffaele, Milan, Italy and Laboratory of Cerebral Metabolism, National Institute of Mental Health, Bethesda, Maryland*

Functional tissue heterogeneity, i.e., inclusion of tissues with different rates of blood flow and metabolism within a single region of interest, is an unavoidable problem with PET. Errors in determination of regional cerebral glucose utilization (rCMRglc) with [$^{18}$F]FDG have resulted from the currently used simplifying assumption that all regions examined are homogeneous. We have established an optimal, yet practical procedure to minimize errors due to tissue heterogeneity in determination of rCMRglc. Effects of applying the three-rate constant kinetic model designed for homogeneous tissues with both dynamic and single-scan procedures and the Patlak plot were evaluated in normal subjects in experimental periods up to 120 min following tracer injection. The procedure with a single scan carried out any time within the interval between 60 and 120 min following tracer injection, combined with population average rate constants determined over a 120-min period, was found to be optimal for quantitative rCMRglc studies.

**J Nucl Med 1993; 34:360–369**

Two different compartmental models are currently used for quantification of regional cerebral glucose utilization (rCMRglc) with 2-[$^{18}$F]fluoro-2-deoxy-D-glucose (FDG) and positron emission tomography (PET): the 3K model that includes three rate constants and assumes that dephosphorylation of [$^{18}$F]fluorodeoxyglucose-6-phosphate (FDG-6-P) during the experimental period is negligible (*1*) and the 4K model that includes an additional first-order rate constant to correct for assumed dephosphorylation of [$^{18}$F]FDG-6-P (*2*). Both models apply only to localized regions of tissue that are homogeneous with respect to rates of blood flow, rates of transport of [$^{18}$F]FDG and glucose between plasma and tissue, concentrations of [$^{18}$F]FDG, glucose, [$^{18}$F]FDG-6-P, and glucose-6-phosphate, and rate of glucose utilization. Whereas such conditions can be reasonably well approached in quantitative autoradiographic studies that permit selective placement of small regions of interest (ROIs), they cannot be realized in PET studies due to the limited spatial resolution of emission tomography. Indeed, a comparison of PET and magnetic resonance images illustrates the degree to which structural heterogeneity, i.e. inclusion of both gray and white matter in a ROI, is unavoidable in PET. Because the gray and white matter tissues have different rates of blood flow and metabolism, this implies functional heterogeneity in the ROI as well. Furthermore, gray matter itself may be comprised of metabolically diverse tissues. Functional, i.e., kinetic, heterogeneity is always present even with PET scanners that have very high spatial resolution.

When the kinetic models designed for homogeneous tissues are applied to heterogeneous tissues, the rate constant for efflux of [$^{18}$F]FDG from tissue to plasma, $k_2^*$, and the rate constant for phosphorylation of [$^{18}$F]FDG to [$^{18}$F]FDG-6-P in the tissue, $k_3^*$, are overestimated at early times (*3,4*). The estimates of these rate constants decline with time and approach constant levels that equal their true mass-weighted average values only at long experimental times when the various tissue pools in the mixed tissue equilibrate with the arterial plasma (*3,4*). After such equilibration, average values for rCMRglc in the brain as a whole obtained with the 3K model were shown to agree very closely with values obtained with the Kety-Schmidt technique (*4*). When the 4K model was applied to heterogeneous tissues, however, estimates of the rate constant for dephosphorylation of [$^{18}$F]FDG-6-P, $k_4^*$, were artifactually high and rCMRglc was consistently overestimated by more than 20% in all experimental periods up to 120 min after a pulse of [$^{18}$F]FDG (*4*). We

Received Jun. 2, 1992; revision accepted Nov. 4, 1992.

For correspondence or reprints contact: G. Lucignani, MD, INB-CNR, Dept. of Nuclear Medicine, University of Milan, c/o Institute H. San Raffaele, Via Olgettinga, 60, I-20132 Milan, Italy.

concluded that the 4K model is not accurate with experimental periods of 120 min or less.

Procedures based on these kinetic models are implemented with either a single 10–15 min brain scan beginning after a delay to allow tracer uptake (i.e., "single-scan" procedure) with rate constants determined in separate matched populations (*2,5*) or with a series of consecutive scans beginning at the time of tracer injection (i.e., "dynamic" procedure) (*6*). It has been generally assumed that the dynamic procedure provides more accurate estimates of rCMRglc because the rate constants are determined for each individual subject and ROI at the time of the study (*6,7*).

The multiple-time graphical analysis technique (i.e., "Patlak plot") is also used for determination of rCMRglc (*8,9*) and has the advantage of applying to both homogeneous and heterogeneous tissues (*10*). It requires that a series of scans be carried out after equilibration of all the free [$^{18}$F]FDG pools in the tissue with the plasma, but before any loss of product occurs. Application of this technique is somewhat limited by the difficulty in objectively identifying the appropriate scanning times.

In the heterogeneous tissues examined by PET, minimization of errors due to incomplete equilibration of tissues with the plasma becomes critical for the determination of rCMRglc by both the compartmental approach and the Patlak plot. Equilibrium between brain and plasma may not yet be achieved as late as 60 min following administration of [$^{18}$F]FDG (*4*). This implies that since scanning must be carried out from the time of tracer administration through a period in which equilibrium is maintained to obtain true mass-weighted average rate constants in heterogeneous tissue, dynamic protocols will require prolonged scanning procedures. The alternative is to use a single-scan procedure that allows shorter scanning times, but must be designed to be minimally sensitive to deviations in the individual's rate constants from the standard set of rate constants derived from a matched population.

The purpose of the current study was to establish an optimal yet practical procedure for determination of rCMRglc in heterogeneous tissues with [$^{18}$F]FDG and PET. We have determined rCMRglc at various time intervals up to 120 min following a pulse of [$^{18}$F]FDG in order to define: (1) the most suitable time frame for determination of rate constants and rCMRglc with the 3K model by the dynamic procedure; (2) the set of rate constants and best time frame for determination of rCMRglc with the 3K model and single-scan procedure; and (3) the time frame for determination of rCMRglc with the Patlak plot.

## MATERIALS AND METHODS

### Subjects

Four human subjects (3 male and 1 female, mean age 34 yr, range 26–42 yr), healthy and normal as determined by medical and neurological examination, were studied. Prior to the PET studies, the subjects signed an informed consent describing the purpose and risks of the study. Permission for the study was issued by the Ethics Committee of the Institute H. San Raffaele, Milan, Italy.

### PET Studies

The synthesis of [$^{18}$F]FDG was carried out according to the method of Hamacher et al. (*11*) as previously described (*4*). PET scans were performed with a four-ring whole body positron emission tomograph (Model 931/04-12; Siemens/CPS, Knoxville, TN). Subjects were in a resting state with eyes open and ears unplugged. Each study was started with insertion under local anesthesia of a 20-gauge teflon catheter into a radial artery. Subjects were then positioned on the scanner bed with their heads immobilized by a customized head-holder. Positioning of the subject's head was achieved with the aid of laser beams and skin marks. One 10-min transmission scan was carried out with an external $^{68}$Ge ring source. Each subject then received an intravenous pulse of 7–10 mCi of [$^{18}$F]FDG. Simultaneous acquisition of data from seven equally spaced transaxial planes (4 direct and 3 cross planes; slice thickness, 6.75 mm) parallel to the orbital-meatal line, including structures between the basal ganglia and the centrum semiovale covering an axial field of view of 5.4 cm was carried out. Scanning proceeded continuously according to the following schedule: 5 scans of 1 min each, 5 scans of 2 min each and 21 scans of 5 min each for a total scanning time of 120 min. In one subject, scanning was stopped at 80 min. Timed arterial blood samples were collected continuously for the first minute following the [$^{18}$F]FDG administration and then at increasing intervals up to the end of the PET scanning. They were rapidly centrifuged and glucose and $^{18}$F concentrations were assayed in the plasma. Scans were reconstructed with a Hann filter with a cut-off frequency of 0.5 cycles per pixel. Under these conditions, the spatial resolution in the image plane was 8 mm full width at half-maximum (FWHM). Each image was reconstructed on a 128 × 128 matrix with a pixel size of 1.56 mm. Correction for attenuation of the 512-keV annihilation gamma rays by the tissue was performed with the coefficients obtained from the transmission scan. Thirty-one discrete anatomical ROIs were drawn on the image from the final emission scan (Fig. 1) and then transferred to the images from each of the other emission scans to obtain the time course of total radioactivity in each ROI. In addition, whole brain total radioactivity was determined as the weighted average of the radioactivity in the seven image planes. For determination of rate constants and rCMRglc with the compartmental model, total radioactivity measured by the PET scanner was corrected for radioactivity in the blood as previously described (*4*). A value of 3% was assumed to be the blood-to-tissue weight ratio for the whole brain, the cortical ribbon and the subcortical gray matter. A value of 2% was assumed for white matter. No correction for blood volume was applied for the Patlak plot. Plasma glucose concentration was relatively constant throughout each study; it never deviated from the individual mean value by more than ±9%. Mean plasma glucose levels ranged from 0.83 to 0.89 mg/ml among the subjects.

### Rate Constant Estimation

Rate constants were estimated from the differential equations derived from the model that describes the changes in concen-


**FIGURE 1.** PET image of the plane 8.2 cm above the orbital-meatal line, obtained during the 115–120-min interval following a pulse of [$^{18}$F]FDG, shows placement of ROIs on the cortical ribbon and in the white matter for one subject. Thirty-one ROIs that were defined according to the atlas of Damasio and Damasio (*16*) and one ROI for the whole brain were examined.

trations of [$^{18}$F]FDG, [$^{18}$F]FDG-6-P and total radioactivity in the tissues (*1*). For each ROI, a weighted nonlinear least squares procedure, according to the Levenberg-Marquardt method (*13*), was used to estimate the rate constants from the total tissue radioactivity data for 22 time intervals, i.e., 0–15 min, 0–20 min, 0–25 min, . . . up to 0–120 min. Weighting factors were the estimated standard deviations of the total tissue radioactivity concentrations (*14*). Arterial plasma [$^{18}$F]FDG concentrations were linearly interpolated between samples. Differential equations were numerically solved by the use of a fourth-order Runge-Kutta procedure with adaptive stepsize control (*13*).

### rCMRglc Determination with Compartmental Model and Dynamic Equation

The equation used for calculation of rCMRglc at any time, T, was that of Huang et al. (*6*):

$$\text{rCMRglc}(T) = [K_1^*k_3^*/(k_2^* + k_3^*)][C_P/LC], \qquad \text{Eq. 1}$$

where $K_1^*$, $k_2^*$, and $k_3^*$ are the rate constants estimated for each individual subject and each ROI, including the whole brain, for the time interval ending T min after injection of tracer, $C_P$ is the arterial plasma glucose concentration and LC is the lumped constant. A value of 0.52 was used for the LC (*15*).

### rCMRglc Determination with Compartmental Model and Single-Scan Equation

rCMRglc at any time T was calculated by the equation of Sokoloff et al. (*1*):

$$\text{rCMRglc}(T) = \frac{C_i^*(T) - K_1^* e^{-(k_2^* + k_3^*)T} \int_0^T C_P^*(t) e^{(k_2^* + k_3^*)t}\, dt}{LC\left[\int_0^T [C_P^*(t)/C_P]\, dt - e^{-(k_2^* + k_3^*)T} \int_0^T [C_P^*(t)/C_P] e^{(k_2^* + k_3^*)t}\, dt\right]}, \qquad \text{Eq. 2}$$

where $C_i^*(T)$ is the measured total tissue radioactivity in the ROI at time T, $K_1^*$, $k_2^*$, $k_3^*$, LC and $C_P$ are defined as above and $C_P^*(t)$ is the concentration of [$^{18}$F]FDG in plasma at time t. rCMRglc was calculated with two sets of rate constants: (1) those determined from dynamic scans of each ROI, including the whole brain, in each individual subject for the time interval ending T min after injection of tracer and (2) the mass-weighted average rate constants for both gray and white matter determined in three subjects over the entire time course of the studies (0–120 min), the interval that provides estimates for the rate constants of each ROI closest to their true mass-weighted average values. The value of the LC was 0.52 as in Equation 1.

### rCMRglc Determination with the Multiple Time-Graphical Technique (Patlak Plot)

After an initial period of equilibration between the pools of free [$^{18}$F]FDG in the tissues and plasma, the slope of the plot of $C_i^*(T)/C_P^*(T)$ versus $\int_0^T C_P^*(t)\, dt/C_P^*(T)$ becomes linear with a constant slope K (*8,9*), equal to $K_1^*k_3^*/(k_2^* + k_3^*)$ for a homogeneous tissue or the mass-weighted average of this combination of rate constants for a heterogeneous tissue (*10*), as long as there is no significant loss of metabolic product. rCMRglc can then be calculated as:

$$\text{rCMRglc} = KCp/LC. \qquad \text{Eq. 3}$$

Application of this method requires identification of an appropriate time interval during which the graph is truly linear. Lack of linearity can be due to incomplete equilibration between tracer in plasma and tissue, loss of metabolic product, or both. Lack of equilibration is of greatest relevance at early times whereas loss of product should be most relevant at later times. There is not yet a convenient, objective method for identifying the most appropriate time interval when complete equilibration is assured and the value of K may depend on the interval chosen. To identify such an interval, we determined K for 48 time intervals between 15 and 120 min and searched for an interval in which K remained relatively constant. The intervals examined consisted of eighteen 20-min intervals (i.e., 15–35 min, 20–40 min, . . . , 100–120 min), sixteen 30-min intervals (i.e., 15–45 min, 20–50 min, . . . , 90–120 min), and fourteen 40-min intervals (i.e., 15–55 min, 20–60 min, . . . , 80–120 min). rCMRglc was computed for each interval by Equation 3.

### Statistical Analyses

Values of rCMRglc calculated with mass-weighted average rate constants and the single-scan procedure were tested for statistically significant differences by one-way analysis of variance (ANOVA). Data from scans carried out in the intervals 30–40 min, 40–50 min, 50–60 min, 60–75 min, 75–90 min, 90–105 min and 105–120 min following tracer injection were compared. The same test was used for the statistical analysis of values of rCMRglc obtained with the Patlak plot during six 30-min time intervals between 30 and 120 min. In this case, the statistical analysis was carried out on two independent sets of data (i.e., data collected between 15–45 min, 45–75 min, 75–105 min and data collected between 30–60 min, 60–90 min, 90–120 min).

## RESULTS

### Rate Constants Determined with Compartmental Model

When the rate constants were determined for every time interval in every ROI, estimates of the rate constant for influx of [$^{18}$F]FDG from plasma to tissue, $K_1^*$, fell

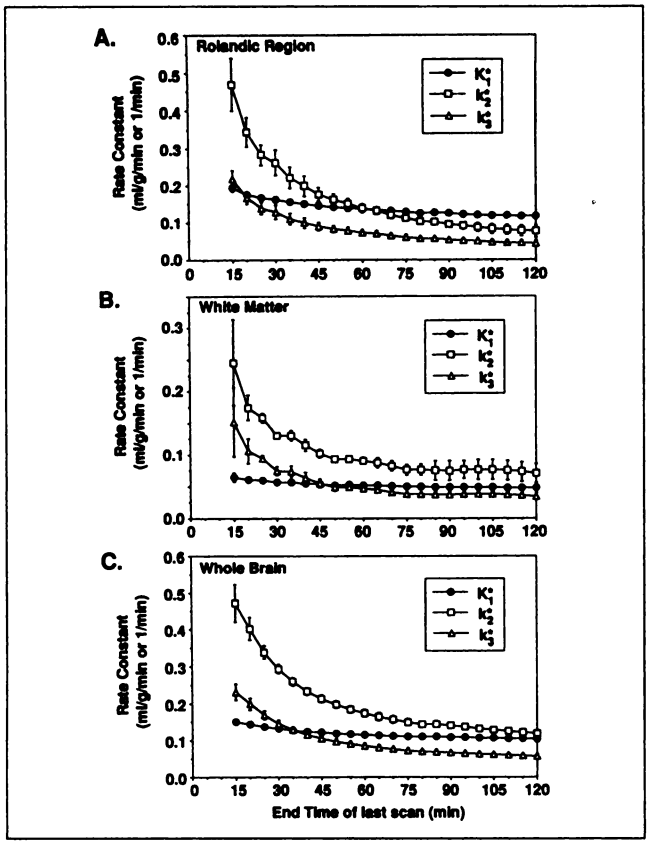


**FIGURE 2.** Time courses of the rate constants $K_1^*$, $k_2^*$, and $k_3^*$ estimated with the 3K model. (A) Rate constants estimated from the total tissue radioactivity measured in one representative gray matter region in the interval beginning with the pulse of [$^{18}$F]FDG and ending at the time indicated on the abscissa. Values are the means ± s.e.m. for four subjects for the intervals ending between 15 and 80 min, and for three subjects for the intervals ending between 85 and 120 min. (B) Corresponding values in white matter. (C) Corresponding values for whole brain. The estimates of $k_2^*$ and $k_3^*$ initially fall sharply as the duration of the fitting interval is increased and tend to level off later in the experimental period. This is consistent with the time variability expected to occur in a heterogeneous tissue (*3,4*).

slightly with time. On the other hand, estimates of the rate constants for efflux of [$^{18}$F]FDG from tissue to plasma and for phosphorylation of [$^{18}$F]FDG in the tissue, $k_2^*$ and $k_3^*$, respectively, initially declined sharply but then became relatively constant with long fitting intervals. The time courses of the estimates of the rate constants are illustrated for two representative ROIs and whole brain in Figure 2. The asymptotic values of the rate constants, i.e., those determined over the 0–120-min interval, for 14 representative gray and one white ROIs are listed in Table 1. Since the asymptotic values of the rate constants represent the mass-weighted average rate constants for each ROI, even in heterogeneous regions (*3*), but it is possible to calculate the mass-weighted average rate constants for the gray and white matter structures studied. These values are also listed in Table 1 along with the rate constants determined for the whole brain treated as a single ROI.

### rCMRglc Determined with Compartmental Model and Dynamic Procedure

rCMRglc was calculated from the dynamic scans according to Equation 1 with rate constants determined for each ROI, each individual subject and each time interval. The values for rCMRglc declined with time with short experimental periods and became relatively constant only after approximately 60 min and remained so throughout the remainder of the 120 min experimental period. The time courses of calculated rCMRglc in two representative ROIs and in whole brain are shown in Figure 3A. rCMRglc was also calculated according to Equation 2 with the same rate constants, i.e., those determined from the dynamic scans for each ROI, each individual subject and each time interval (Fig. 3B). rCMRglc calculated according to Equation 2 was in complete agreement with the values obtained with Equation 1 (Fig. 3C).

### rCMRglc Determined with Compartmental Model and Single-Scan Procedure

When rCMRglc was calculated at various times following the pulse of [$^{18}$F]FDG with the asymptotic mass-weighted population average rate constants, i.e., with the average of the rate constants determined over the interval 0–120 min in the three subjects from this study, it became constant approximately 30 min after tracer injection, which was much sooner than when calculated with rate constants specific for each region, subject and time interval. The time course of calculated rCMRglc for two representative ROIs and whole brain is shown in Figure 4. The values for rCMRglc in representative ROIs calculated with asymptotic average gray and average white matter rate constants are given in Table 2. Statistically significant differences in the values calculated at the different time intervals were observed in only two of the 31 regions examined and in the whole brain.

### rCMRglc Determined by the Multiple Time-Graphical Technique (Patlak Plot)

When time intervals that were 20 min long (i.e., 4 points on the graph of $C_i^*(T)/C_P^*(T)$ versus $\int_0^T C_P^*(t)\,dt/C_P^*(T)$) were used to fit a straight line and determine the slope (i.e., K) of the Patlak plot, many linear segments of the curve were identified with similar goodness-of-fit. Five 20-min linear segments between 15–35 min and 95–115 min that were fitted to scan data from the whole brain and two representative ROIs in one subject are shown in Figure 5A. A different value of K and, therefore, corresponding value of rCMRglc was found for each interval (Fig. 5B). For example, rCMRglc varied from 26–35 μmol/100g/min for whole brain. When time intervals of 30 or 40 min duration (i.e., 6 and 8 points, respectively) were used to fit a straight line, many of the linear segments over these ranges of the curve were also found to have

**TABLE 1**
Rate Constants Determined with 3K Model in Representative Gray and White Matter Regions*

| Region | $K_1^*$ (ml/g/min) | $k_2^*$ ($min^{-1}$) | $k_3^*$ ($min^{-1}$) |
|---|---|---|---|
| Cingulate gyrus | 0.114 ± 0.005 | 0.069 ± 0.010 | 0.043 ± 0.004 |
| Supplementary motor area | 0.111 ± 0.007 | 0.080 ± 0.011 | 0.045 ± 0.007 |
| Prefrontal region | 0.103 ± 0.006 | 0.072 ± 0.014 | 0.040 ± 0.005 |
| Rolandic region | 0.117 ± 0.008 | 0.076 ± 0.015 | 0.044 ± 0.007 |
| Frontal operculum | 0.102 ± 0.004 | 0.073 ± 0.005 | 0.049 ± 0.006 |
| Premotor region and rolandic region | 0.101 ± 0.003 | 0.073 ± 0.002 | 0.046 ± 0.004 |
| Head of caudate | 0.081 ± 0.002 | 0.052 ± 0.008 | 0.032 ± 0.005 |
| Infracalcarin cortex | 0.126 ± 0.011 | 0.092 ± 0.022 | 0.045 ± 0.011 |
| Supracalcarin cortex | 0.113 ± 0.004 | 0.082 ± 0.008 | 0.045 ± 0.006 |
| Occipital cortex | 0.092 ± 0.002 | 0.053 ± 0.001 | 0.036 ± 0.002 |
| Middle temporal gyrus | 0.101 ± 0.004 | 0.066 ± 0.009 | 0.038 ± 0.002 |
| Inferior temporal gyrus | 0.098 ± 0.003 | 0.068 ± 0.005 | 0.039 ± 0.004 |
| Auditory cortex | 0.089 ± 0.008 | 0.069 ± 0.018 | 0.039 ± 0.007 |
| Thalamus | 0.092 ± 0.010 | 0.052 ± 0.019 | 0.026 ± 0.007 |
| Weighted average gray matter | 0.101 | 0.071 | 0.042 |
| White matter | 0.047 ± 0.003 | 0.070 ± 0.015 | 0.035 ± 0.005 |
| Whole brain | 0.104 ± 0.001 | 0.118 ± 0.004 | 0.056 ± 0.006 |

*Determined over the interval 0–120 min. Values are means ± s.e.m. for three subjects.

similar goodness-of-fit. The slope of the linear segments varied with the interval chosen and the general trend was for the K (i.e., the Patlak slope) to decline initially with the ending time of the interval until more than 75 min following injection of the [$^{18}$F]FDG. The trend, however, usually reversed and the slope actually increased temporarily for some intervals that ended between approximately 75 and 105 min. In the late intervals that ended between approximately 105 and 120 min, the values of K again decreased. Although the changes in rCMRglc were often not statistically significant (see below), the decrease-increase-decrease pattern was consistent; it occurred in approximately two-thirds of the ROIs examined. Results for two representative ROIs and for the whole brain are shown in Figure 6. The magnitude of the fluctuations in the estimated Ks was highest when the 20-min segments were used in fitting; somewhat lower with the 30-min segments; and lowest with the 40-min segments (Fig. 6). rCMRglc calculated from the slope of the Patlak Plot determined from various 30-min segments is given in Table 3. Statistically significant differences ($p < 0.05$) in the values for rCMRglc calculated between 15–45 min, 45–75 min and 75–105 min were observed in 6 of the 31 ROIs examined and in the whole brain. Statistically significant differences ($p < 0.05$) were also found in two gray ROIs and in the white matter when rCMRglc was calculated for the intervals 30–60 min, 60–90 min and 90–120 min. To test whether these significant differences were due only to the data at early times, we compared the values obtained for the interval 45–75 min with those obtained at 75–105 min and the values obtained at 60–90 min with those at 90–120 min. Statistically significant differences ($p < 0.05$) were found in only one gray structure between the values at 45–75 min and 75–105 min and only in the white matter between 60–90 min and 90–120 min.

## DISCUSSION

The [$^{18}$F]FDG method has been used extensively to measure rCMRglc in man with emission tomography since its introduction in 1979 (*2,5*). During the prolonged scanning periods required with the early generation of PET scanners, total tissue radioactivity in brain was observed to decline after approximately 120 min resulting in progressive lowering of calculated rCMRglc. This phenomenon was arbitrarily attributed to dephosphorylation of [$^{18}$F]FDG-6-P and led to the introduction of the 4K model (*2*). With current scanners, it is possible to measure the time courses of rapidly changing tissue concentrations of radioactivity simultaneously in several image planes with dynamic or single-scan procedures and data acquisitions over a period of time much shorter than previously necessary. If the entire experimental period is kept within 120 min, a period in which there is no direct evidence of any significant product loss, there is no obvious reason to use the 4K model (*3,4*). Furthermore, we showed in a previous study that the use of the 4K model leads to overestimation of rCMRglc when scanning is completed within 120 min (*4*). Therefore, we have restricted our analyses in the present study to data acquired within a 120-min experimental period when $k_4^*$ models are unnecessary. In the current study, we found that rCMRglc calculated with the 3K model remained fairly constant between 30 and 120 min when an appropriate set of rate constants was used. If there were any significant loss of product during this time period, the calculated rCMRglc

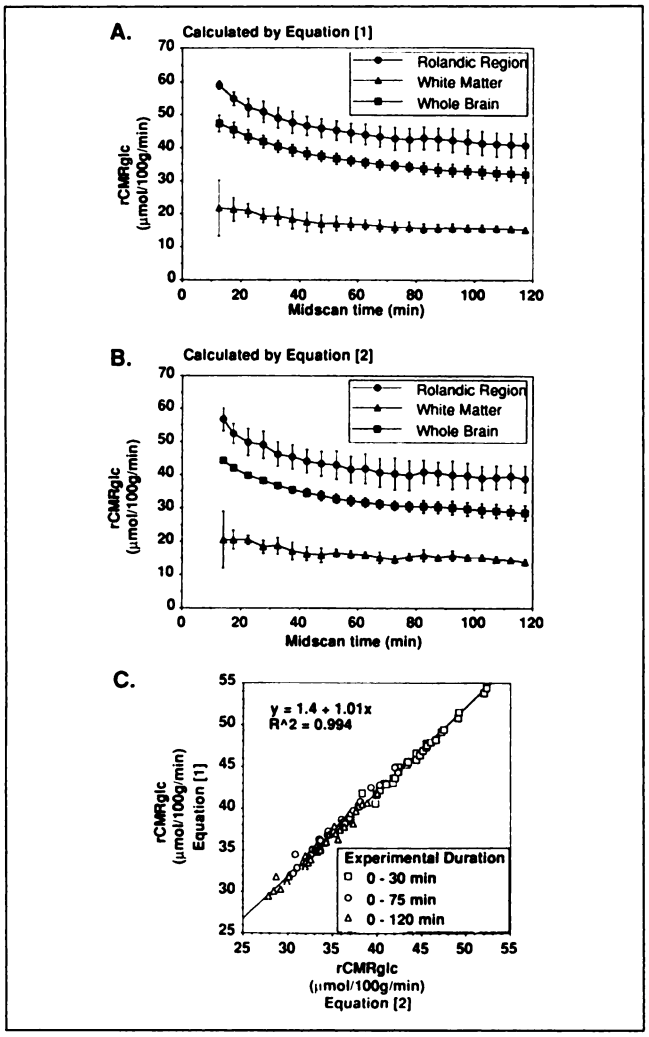


**FIGURE 3.** Time courses of rCMRglc calculated with Equations 1 and 2, with rate constants determined during dynamic scans of each ROI, including the whole brain, in each subject for each time interval. (A) Values of rCMRglc calculated with Equation 1 from the total tissue radioactivity measured in one gray matter structure, one white structure and whole brain in the interval beginning with the pulse of [$^{18}$F]FDG and ending at the time indicated on the abscissa. Values are the means ± s.d. for four subjects in the intervals ending between 15 and 80 min, and for three subjects in the intervals ending between 85 and 120 min. (B) Corresponding values of rCMRglc calculated with Equation 2. With both methods of calculation the values of rCMRglc initially fall as the end of the scanning time is increased and tend to level off later in the experimental period. This is consistent with the time variability expected to occur in a heterogeneous tissue (*3,4*). (C) Correlation between values of rCMRglc calculated with Equation 1 (ordinate) and with Equation 2 (abscissa) at various times following a pulse of [$^{18}$F]FDG. Each point represents rCMRglc in one ROI.

should fall inasmuch as the 3K model does not correct for any loss of product.

It is generally believed that dynamic methods in association with compartmental models provide estimates of rCMRglc that are more accurate than those obtained with single-scan methods because the model rate constants are determined specifically for the individual subject and ROIs at the time of the study (*6,7*). Dynamic methods may not be more accurate, however, when the underlying compartmental model does not adequately reflect the true kinetic behavior of the tracer in the tissue. For example, when a kinetic model designed for homogeneous tissues is applied to heterogeneous tissues, the rate constants determined prior to achievement of tissue to plasma equilibrium do not represent mass-weighted average rate constants for the mixed tissue in the ROI (*3,4*). Following an intravenous pulse of [$^{18}$F]FDG, equilibration is never completely achieved, but sufficient equilibration can be assumed in all regions when the estimates of the rate constants become relatively constant with time. It remained to be shown whether rate constants determined prior to equilibrium for individual heterogeneous regions were indeed more appropriate than average population mass-weighted rate constants determined at longer times.

In this study, we have shown that rate constants determined in each individual region and subject prior to achievement of sufficient equilibration decline with time. The use of rate constants determined at experimental times shorter than 60 min produces errors in the estimated rates of glucose consumption. These errors are avoided by the use of mass-weighted average population rate constants determined at longer experimental times. Moreover, the values determined for rCMRglc become constant for most ROIs at about 30 min after the pulse when the mass-weighted average population rate constants determined at 120 min are used. The use of either the dynamic procedure or the single-scan procedure with population average rate constants for

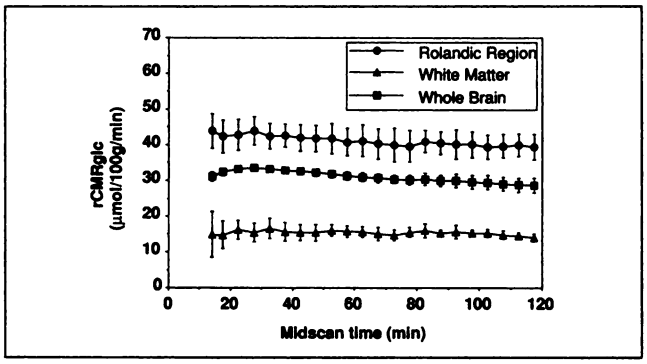


**FIGURE 4.** Time courses of rCMRglc calculated with Equation 2 and mass-weighted average population rate constants reported in Table 1 (average gray: $K_1^* = 0.101$, $k_2^* = 0.071$, $k_3^* = 0.042$; average white: $K_1^* = 0.047$, $k_2^* = 0.070$, $k_3^* = 0.035$; whole brain: $K_1^* = 0.104$, $k_2^* = 0.118$, $k_3^* = 0.056$). rCMRglc was calculated from the total tissue radioactivity measured in whole brain, in one gray matter structure and in white matter, during each of 22 5-min scans. The midscan time of each measurement is indicated on the abscissa. Values are the means ± s.d. calculated for four subjects in the intervals ending between 15 and 80 min and for three subjects in the intervals ending between 85 and 120 min. The calculated values of rCMRglc tend to fall very slightly with time as the interval between tracer injection and the time at which the scan is performed increases.

**TABLE 2**
Regional rCMRglc Calculated with the 3K Model and the Single-Scan Procedure in Representative Gray and White Matter Regions*

| Region | rCMRglc (μmol/100 g/min) | | | | | | |
|---|---|---|---|---|---|---|---|
| | Scan start-stop time (min) | | | | | | |
| | 30–40 (n = 4) | 40–50 (n = 4) | 50–60 (n = 4) | 60–75 (n = 4) | 75–90 (n = 3) | 90–105 (n = 3) | 105–120 (n = 3) |
| Cingulate gyrus | 45 ± 2 | 45 ± 2 | 43 ± 3 | 43 ± 3 | 42 ± 2 | 42 ± 3 | 41 ± 3 |
| Supplementary motor area | 39 ± 1 | 39 ± 2 | 38 ± 2 | 37 ± 2 | 37 ± 3 | 38 ± 3 | 36 ± 3 |
| Prefrontal region | 37 ± 1 | 37 ± 2 | 36 ± 2 | 36 ± 1 | 35 ± 1 | 35 ± 1 | 34 ± 2 |
| Rolandic region | 42 ± 3 | 42 ± 4 | 41 ± 4 | 40 ± 4 | 41 ± 3 | 40 ± 4 | 40 ± 3 |
| Frontal operculum | 40 ± 2 | 39 ± 2 | 38 ± 2 | 38 ± 1 | 38 ± 2 | 38 ± 3 | 37 ± 3 |
| Premotor region and rolandic region | 38 ± 1 | 37 ± 1 | 37 ± 1 | 36 ± 1 | 37 ± 1 | 36 ± 1 | 35 ± 1 |
| Head of caudate | 31 ± 4 | 31 ± 2 | 31 ± 3 | 31 ± 1 | 30 ± 2 | 29 ± 2 | 28 ± 2 |
| Infracalcarin cortex | 43 ± 5 | 42 ± 5 | 41 ± 5 | 40 ± 5 | 40 ± 6 | 40 ± 7 | 38 ± 6 |
| Supracalcarin cortex† | 40 ± 1 | 40 ± 1 | 39 ± 0 | 38 ± 0 | 37 ± 1 | 37 ± 1 | 36 ± 1 |
| Occipital cortex† | 37 ± 2 | 37 ± 1 | 37 ± 1 | 36 ± 1 | 35 ± 1 | 35 ± 1 | 34 ± 1 |
| Middle temporal gyrus | 37 ± 4 | 37 ± 3 | 37 ± 3 | 36 ± 3 | 35 ± 4 | 35 ± 4 | 34 ± 4 |
| Inferior temporal gyrus | 36 ± 2 | 36 ± 2 | 35 ± 2 | 34 ± 2 | 34 ± 2 | 33 ± 3 | 33 ± 3 |
| Auditory cortex | 29 ± 4 | 30 ± 4 | 30 ± 5 | 31 ± 4 | 30 ± 3 | 30 ± 3 | 30 ± 4 |
| Thalamus | 35 ± 4 | 35 ± 4 | 35 ± 4 | 33 ± 3 | 33 ± 3 | 30 ± 3 | 31 ± 4 |
| White matter | 16 ± 3 | 15 ± 2 | 16 ± 2 | 15 ± 2 | 16 ± 1 | 15 ± 1 | 14 ± 1 |
| Whole brain† | 34 ± 1 | 33 ± 1 | 32 ± 1 | 32 ± 1 | 31 ± 2 | 31 ± 2 | 30 ± 2 |

*Calculated with mass-weighted average rate constants determined in the interval 0–120 min (gray matter: $K_1^* = 0.101$ ml/g/min, $k_2^* = 0.071$ min$^{-1}$, $k_3^* = 0.042$ min$^{-1}$; white matter: $K_1^* = 0.047$ ml/g/min, $k_2^* = 0.070$ min$^{-1}$, $k_3^* = 0.035$ min$^{-1}$; whole brain: $K_1^* = 0.104$ ml/g/min, $k_2^* = 0.118$ min$^{-1}$, $k_3^* = 0.056$ min$^{-1}$). rCMRglc values are means ± s.d. for the number of subjects indicated.
†Values determined in the different time intervals are statistically significantly different (ANOVA, $p < 0.05$).

times when the values for rCMRglc become relatively stable (e.g., >60 min) yields similar results. Therefore, there is no reason to use a dynamic protocol that requires a scanning procedure in which the subject must remain positioned and motionless in the scanner for at least 60 min when a single scan lasting only 10–15 min is adequate for calculating rCMRglc. In this study, a set of average rate constants for calculation of rCMRglc was applied to the same population in which it was determined. This set of average rate constants may have led to values of rCMRglc that are more accurate at early times, when calculated rCMRglc is most sensitive to errors in the rate constants, than if they were applied to a different population. The effects of inaccuracies in the rate constants can be minimized, however, by increasing the delay between the administration of [$^{18}$F]FDG and the time of scanning, at least up to 120 min.

Tissue heterogeneity is not a limitation when rCMRglc is calculated by the multiple time-graphical analysis technique of Patlak (*8,9*). This technique requires the determination of an optimal time frame for the scanning procedure after equilibration between tissue and plasma is achieved. Complete equilibration is never fully achieved, however, because the plasma concentration of [$^{18}$F]FDG continues to decline throughout the experimental period. Early declines in rCMRglc calculated by the Patlak plot cannot be attributed to loss of product inasmuch as these declines usually reverse. Increases in calculated rCMRglc begin sometime between 75 and 105 min, depending on the ROI. There should be no such reversal of the decline in calculated rCMRglc if the decline were due to product loss. A more likely explanation for the early declines in calculated rCMRglc is that sufficient tissue to plasma equilibration has not yet been achieved. This is consistent with the observations that the kinetic model rate constants do not become relatively constant before 60 min.

Finally, the values obtained with the technique of Patlak tended to be somewhat lower, approximately 10%–15%, than those calculated with the 3K model when mass-weighted average rate constants determined at 120 min were used. The lower estimates of rCMRglc obtained with the Patlak plot than with the 3K model are partially due to the use of a blood volume correction with the 3K model analysis as previously described (*4*). This leads to approximately a 3% difference between the two methods. An additional 1%–2% underestimation can be attributed to the lack of equilibration of unmetabolized [$^{18}$F]FDG between brain tissue and plasma. The rate of clearance of free [$^{18}$F]FDG from the tissue is greater than that from plasma, thus contributing a negative component to the slope of the Patlak plot that leads to a lower value of

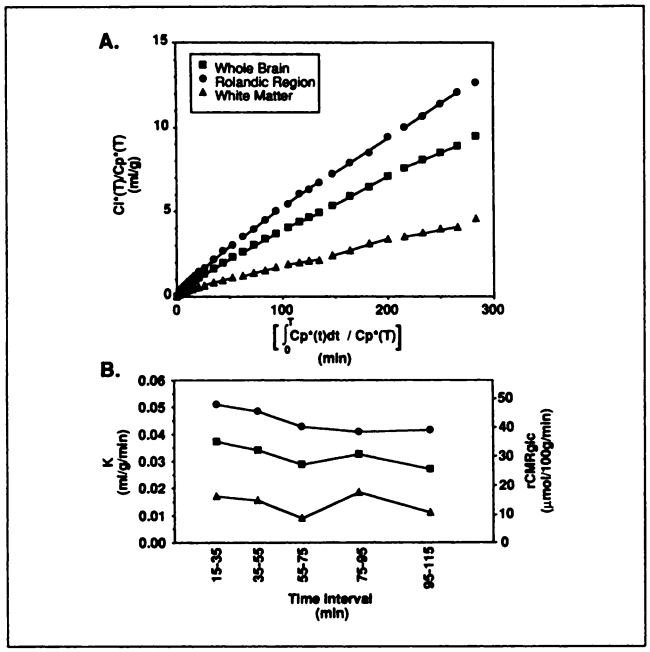


**FIGURE 5.** "Patlak plots" of data obtained during scanning from 0 to 120 min following a pulse of [$^{18}$F]FDG for the whole brain, one gray matter structure and one white structure in a representative subject. (A) The graph shows five 20-min discrete linear segments for each of the three ROIs. Each segment was fitted to four consecutive points, starting and ending, respectively, at 15–35 min, 35–55 min, 55–75 min, 75–95 min and 95–115 min. (B) Values of the slopes of each segment of the Patlak plots shown in Fig. 5A. The left ordinate represents K, i.e., the slope of the plot of $C_i^*(T)/C_p^*(T)$ versus $\int_0^T C_p^*(t)\,dt/C_p^*(T)$, and the right ordinate represents rCMRglc calculated by Equation 3. The slopes vary in a nonrandom fashion depending on the interval in which they were determined. In the five time intervals examined, the calculated values of rCMRglc decline between 15 and 75 min in all three ROIs shown. In whole brain and white matter, as in most of the ROIs examined, the rCMRglc actually increases between 75 and 95 min before falling again in the last interval. In the gray matter ROI, rCMRglc remains relatively constant between 55 and 115 min.

rCMRglc. The reasons for the remainder of the underestimation are not clear.

With all three methods, a trend towards a decline of calculated rCMRglc was observed. Values tended to decrease in most regions by approximately 10% in the interval between 30 and 120 min. These decreases were more consistent when the compartmental models were used but fluctuated when the Patlak plot was used. A slight, but not statistically significant, decline in the estimated rates of rCMRglc was observed with all methods between 60 and 120 min, although the values of rCMRglc at all times during that interval were similar to those obtained with the Kety-Schmidt method. The decline in values calculated with the compartmental models could still be due to an overestimation of the values of the rate constants at 120 min, i.e., prior to the achievement of their true asymptotic mass-weighted value. Some loss of metabolic product may also contribute to the decline in calculated rCMRglc, but it is impossible to separate the effects due to errors in the rate constants from those due to product loss. On the basis of the present data, the single-scan protocol seems to provide a wider time frame for the estimation of stable rCMRglc compared to the Patlak protocol and obviates the need for prolonged dynamic scanning periods.

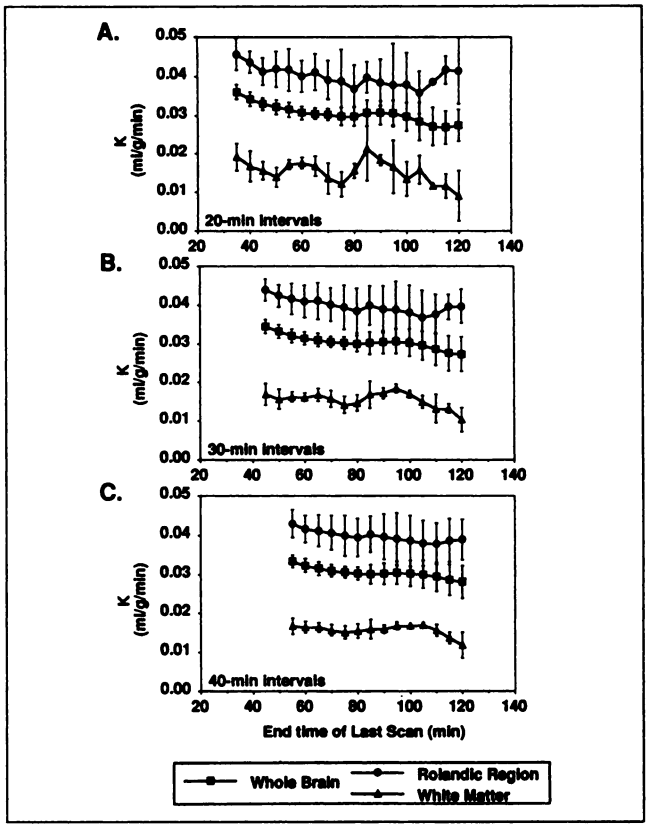


**FIGURE 6.** Slopes of Patlak plots determined from data obtained at different intervals following a pulse of [$^{18}$F]FDG for whole brain and two ROIs. Forty-eight different time intervals between 15 and 120 min following the pulse were examined. The values for the slope (K) are the means ± s.d. for four subjects in the intervals ending between 35 and 80 min and for three subjects in the intervals ending between 85 and 120 min. (A) Values of K (determined from four points on the Patlak plot) for 18 20-min intervals (i.e., 15–35 min, 20–40 min, . . . , 100–120 min). (B) Corresponding values (determined from six points on the Patlak plot) for 16 30-min intervals (i.e., 15–45 min, 20–50 min, . . . , 90–120 min). (C) Corresponding values (determined from eight points on the Patlak plot) for 14 40-min intervals (i.e., 15–55 min, 20–60 min, . . . , 80–120 min). The slope varied with the interval chosen, but the general trend was for the estimated K to decline initially. This trend, however, eventually reversed, and the slope fluctuated thereafter. The fluctuations in the estimated slopes were more evident when the 20-min segments were used in fitting and were somewhat dampened with longer segments.

**TABLE 3**
Regional rCMRglc Calculated with the Patlak Plot in Representative Gray and White Matter Regions*

| Region | rCMRglc (μmol/100 g/min) | | | | | |
|---|---|---|---|---|---|---|
| | Start time of first scan—stop time of last scan (min) | | | | | |
| | 15–45 (n = 4) | 30–60 (n = 4) | 45–75 (n = 4) | 60–90 (n = 3) | 75–105 (n = 3) | 90–120 (n = 3) |
| Cingulate gyrus | 43 ± 3 | 39 ± 4 | 39 ± 3 | 40 ± 3 | 38 ± 7 | 36 ± 3 |
| Supplementary motor area | 39 ± 3 | 36 ± 3 | 33 ± 1 | 35 ± 6 | 37 ± 5 | 31 ± 6 |
| Prefrontal region† | 36 ± 2 | 34 ± 3 | 33 ± 1 | 33 ± 1 | 32 ± 3 | 31 ± 6 |
| Rolandic region | 41 ± 4 | 38 ± 5 | 36 ± 6 | 36 ± 5 | 34 ± 6 | 37 ± 3 |
| Frontal operculum | 39 ± 2 | 35 ± 2 | 35 ± 1 | 36 ± 5 | 36 ± 6 | 33 ± 4 |
| Premotor region and rolandic region† | 38 ± 2 | 35 ± 2 | 33 ± 1 | 35 ± 2 | 33 ± 3 | 31 ± 4 |
| Head of caudate | 33 ± 3 | 30 ± 3 | 29 ± 4 | 30 ± 5 | 24 ± 5 | 24 ± 7 |
| Infracalcarin cortex | 40 ± 5 | 38 ± 6 | 34 ± 3 | 38 ± 9 | 37 ± 11 | 32 ± 5 |
| Supracalcarin cortex† | 40 ± 1 | 36 ± 2 | 33 ± 2 | 34 ± 2 | 34 ± 3 | 31 ± 4 |
| Occipital cortex†‡ | 38 ± 1 | 34 ± 1 | 33 ± 2 | 33 ± 1 | 31 ± 3 | 29 ± 3 |
| Middle temporal gyrus | 37 ± 2 | 35 ± 3 | 32 ± 4 | 31 ± 5 | 30 ± 5 | 28 ± 4 |
| Inferior temporal gyrus | 36 ± 2 | 33 ± 2 | 31 ± 1 | 32 ± 3 | 30 ± 5 | 29 ± 4 |
| Auditory cortex | 32 ± 4 | 29 ± 5 | 29 ± 3 | 27 ± 1 | 29 ± 5 | 26 ± 4 |
| Thalamus | 34 ± 6 | 33 ± 4 | 29 ± 2 | 29 ± 5 | 25 ± 8 | 30 ± 6 |
| White matter‡§ | 16 ± 2 | 15 ± 1 | 13 ± 2 | 16 ± 2 | 14 ± 1 | 10 ± 3 |
| Whole brain† | 32 ± 2 | 29 ± 2 | 28 ± 1 | 28 ± 2 | 27 ± 3 | 25 ± 3 |

*rCMRglc values are means ± s.d. for the number of subjects indicated.
†Values determined in the intervals 15–45, 45–75, and 75–105 min are statistically significantly different (ANOVA, $p < 0.05$).
‡Values determined in the intervals 30–60, 60–90, and 90–120 min are statistically significantly different (ANOVA, $p < 0.05$).
§Values determined in the intervals 60–90, and 90–120 min are statistically significantly different (ANOVA, $p < 0.05$).

## CONCLUSION

Procedures for determination of rCMRglc can rely on the simplest of kinetic models, i.e., the 3K model. Combined with the use of mass-weighted average population rate constants and a single-scan procedure, this model provides accurate values for rCMRglc that remain constant over 1 hr (between 60 and 120 min). Errors due to inaccuracies in the values of the rate constants are minimized by the delay between tracer injection and the scan. Similar results are obtained with the Patlak graphical analysis technique between 45 and 120 min after injection of the tracer. The Patlak technique, however, requires a somewhat longer total scanning time in order to obtain a sufficient number of timed measurements of tracer concentration in the tissue to fit a reliable straight line from which to determine rCMRglc. Both the single-scan and Patlak procedures produce dependable results with shorter scanning times than those required in dynamic procedures in which individual rate constants are fitted.

These results suggest the possibility of using doses of [$^{18}$F]FDG lower than those currently employed. Stability in the estimated rCMRglc over the 60–120-min period indicates that longer scan times within that interval could be used to compensate for lower counting rates in the tissues. Such a procedure would permit reduction of radiation exposure and would be particularly desirable for test-retest protocols that require multiple administrations of radioactivity.


## ACKNOWLEDGMENT

This work was supported in part by CNR Progretto Finalizzato Invecchiamento DNV932255.


## REFERENCES


1. Sokoloff L, Reivich M, Kennedy C, et al. The [$^{14}$C]deoxyglucose method for the measurement of local cerebral glucose utilization: theory, procedure and normal values in the conscious and anesthetized albino rat. *J Neurochem* 1977;28:897–916.
2. Phelps ME, Huang SC, Hoffman EJ, Selin CJ, Sokoloff L, Kuhl DE. Tomographic measurement of local cerebral glucose metabolic rate in humans with [$^{18}$F]2-fluoro-2-deoxy-D-glucose: validation of method. *Ann Neurol* 1979;6:371–388.
3. Schmidt K, Mies G, Sokoloff L. Model of kinetic behavior of deoxyglucose in heterogeneous tissues in brain: a reinterpretation of the significance of parameters fitted to homogeneous tissue models. *J Cereb Blood Flow Metab* 1991;11:10–24.
4. Schmidt K, Lucignani G, Moresco RM, et al. Errors introduced by tissue heterogeneity in estimation of local cerebral glucose utilization with current kinetic models of the [$^{18}$F]fluorodeoxyglucose method. *J Cereb Blood Flow Metab* 1992;12:823–834.
5. Reivich M, Kuhl D, Wolf A, et al. The [$^{18}$F]fluorodeoxyglucose method for the measurement of local cerebral glucose utilization in man. *Circ Res* 1979;44:127–137.
6. Huang SC, Phelps ME, Hoffman EJ, Sideris K, Selin CJ, Kuhl DE. Noninvasive determination of local cerebral metabolic rate of glucose in man. *Am J Physiol* 1980;238:E69–E82.
7. Baron JC, Frackowiak RSJ, Herholz K, et al. Use of PET methods for measurement of cerebral energy metabolism and hemodynamics in cerebrovascular disease. *J Cereb Blood Flow Metab* 1989;9:723–742.

8. Patlak C, Blasberg R. Graphical evaluation of blood-to-brain transfer constants from multiple-time uptake data. Generalizations. *J Cereb Blood Flow Metab* 1985;5:584–590.
9. Patlak C, Blasberg R, Fenstermacher J. Graphical evaluation of blood-to-brain transfer constants from multiple-time uptake data. *J Cereb Blood Flow Metab* 1983;3:1–7.
10. Mori K, Schmidt K, Jay T, et al. Optimal duration of experimental period in measurement of local cerebral glucose utilization with the deoxyglucose method. *J Neurochem* 1990;54:307–319.
11. Hamacher K, Coenen HH, Stocklin G. Efficient stereospecific synthesis of no-carrier-added 2-[$^{18}$F]fluoro-2-deoxy-D-glucose using aminopolyether supported nucleophilic substitution. *J Nucl Med* 1986;27:235–238.
12. Bida GT, Satyamurthy N, Barrio JR. The synthesis of 2-[F-18]fluoro-2-deoxy-D-glucose using glycals: a reexamination. *J Nucl Med* 1984;25:1327–1334.
13. Press WH, Flannery BP, Teukolsky SA, Vetterling WT. *Numerical recipes, the art of scientific computing.* New York: Cambridge University Press; 1986:521–528, 554–560.
14. Budinger TF, Derenzo SE, Greenberg WL, Gullberg GT, Huesman RH. Quantitative potentials of dynamic emission computed tomography. *J Nucl Med* 1978;19:309–315.
15. Reivich M, Alavi A, Wolf A, et al. Glucose metabolic rate kinetic model parameter determination in humans: the lumped constants and rate constants for [$^{18}$F]fluorodeoxyglucose and [$^{11}$C]deoxyglucose. *J Cereb Blood Flow Metab* 1985;5:179–192.
16. Damasio H, Damasio AR. *Lesion analysis in neuropsychology.* New York-Oxford: Oxford University Press; 1989.

## NOTE ADDED IN PROOF

After this paper was submitted, another study concerning the dependency of calculated regional rates of glucose utilization (rCMRglc) on the time of data acquisition appeared in this *Journal* (*1*). Kumar et al. used a kinetic model that assumes first-order dephosphorylation of [$^{18}$F]fluorodeoxyglucose-6-phosphate, i.e. the four rate-constant (4K) model, and a standard population set of rate constants and reported no statistically significant differences in rCMRglc calculated 30 and 45 min after injection of [$^{18}$F]FDG. Kumar et al. then made the implicit assumption that rCMRglc calculated with the 4K model 45 min after injection of [$^{18}$F]FDG was accurate when they concluded that "fluorine-18-FDG PET scans can therefore be reliably performed 30 min after intravenous injection of the radiotracer." We, however, have addressed the questions of both choice of kinetic model and the optimal time frame for each model for determination of rCMRglc in man. In a recent paper (2), we assessed the accuracy of calculated rCMRglc by comparison of the weighted average of rCMRglc values determined in all regions included in the field of view of the PET scanner with whole brain glucose utilization rates determined by the independent Kety-Schmidt technique. We reported that the use of the 4K model leads to overestimation of rCMRglc when scans are performed within 2 hr of tracer injection. Weighted average rCMRglc was more than 20% too high (*2*). We also showed in that study and in the current one that the use of a three rate-constant model leads to more accurate values of rCMRglc provided that it is applied in an experimental period sufficiently long for the effects of tissue heterogeneity to become negligible, but short enough for effects of loss of product to remain insignificant. The current widely used scanning time of 45 min following injection of radiotracer in man has been based on the finding that 45 min is the optimal experimental period in the rat. The optimal time for studies in man had not yet been established. Our present study considered a wide range of possible scanning times between 30 and 120 min after injection of tracer and showed that for both stability and accuracy at least 60 min should be allowed for tracer circulation.

## REFERENCES

1. Kumar A, Braun A, Schapiro M, Grady C, Carson R, Herscovitch P. Cerebral glucose metabolic rates after 30 and 45 minute acquisitions: a comparative study. *J Nucl Med* 1992;33:2103–2105.
2. Schmidt K, Lucignani G, Moresco RM, et al. Errors introduced by tissue heterogeneity in estimation of local cerebral glucose utilization with current kinetic models of [$^{18}$F]flurordeoxyglucose method. *J Cereb Blood Flow Metab* 1992;12:823–834.